CHAPTER 3
MATERIALS AND METHODOLOGY

3.1 Introduction

The present investigation aims to study the behavior of geocell-reinforced foundation systems under static and repeated loading. For this purpose, a series of laboratory model tests were carried out on a specially designed experimental setup in the laboratory. This chapter presents the materials and methodology adopted in different parts of the study.

3.2 Materials used

Geocell reinforcement is commonly used in subgrade soil under various conditions such as soft or loose soil, sloping terrain and erosion control etc. to improve its engineering properties and enhance its performance. The geocells confine the soil particles, increasing their stiffness and strength. This helps to mitigate issues such as settlement, lateral spreading, and soil erosion. The typical geocell-reinforced foundation system used for this study is depicted in Fig. 3.1. It comprises three elements namely geocell reinforcement, infill soil, and existing or filled-up subgrade soil. In practice, geocell pockets are filled with granular materials like sand or gravel which possess higher drainage properties and provide better reinforcement behaviour.

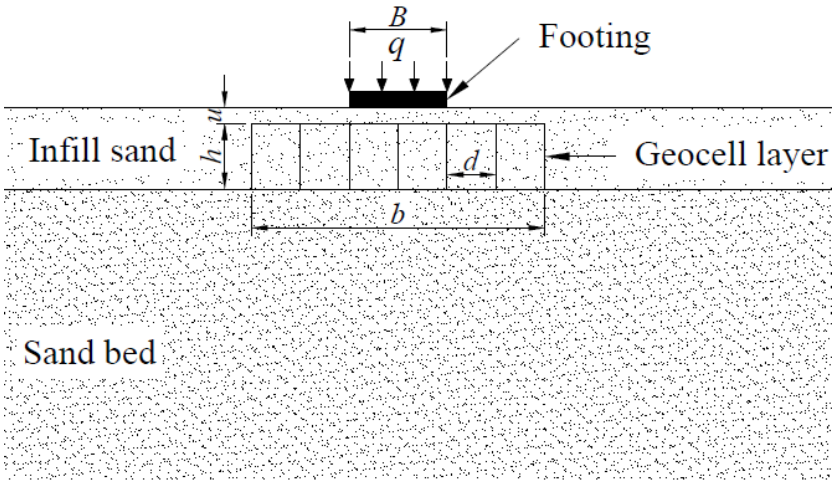

Fig. 3.1 Schematic configuration of geocell-reinforced foundation system

The subgrade soil can be clay or sand at different states of strength/density levels. For the present study, both subgrades and infill soils consisted of sand. A curtain blind was used as geocell reinforcement by stitching in three-dimensional interconnected cells. In this thesis, the nomenclature used for geocell reinforcement is as follows: d – equivalent diameter of geocell pocket; h – the height of geocell reinforcement; u – placement depth of geocell reinforcement from the bottom of the footing; b - width of geocell reinforcement (Fig. 3.1).

3.2.1 Sand

Brahmaputra river sand was used as a base and infill material in this study. The sand was freed of roots, organic matter, etc. through a washing and cleaning procedure. The sample was then air dried (water content ≈ 1%) in the laboratory before it was used in the experimental work. The sand's specific gravity was determined as 2.66 [58]. The density in the densest state was found to be 1730 kg/m^3 and that in the loosest state was 1510 kg/m^3 [56]. The particle size distribution curve obtained from dry sieve analysis is shown in Fig. 3.2 [55]. The physical properties of sand are given in Table 3.1 [53].

Table 3.1 Geotechnical properties of the Brahmaputra river sand used

Materials	**Material properties**	**Values**
Sand (SP)	Specific gravity	2.66
	Effective size, D_{10} (mm)	0.30
	Mean particle size, D_{50} (mm)	0.60
	Coefficient of uniformity (C_u)	2.33
	Coefficient of curvature (C_c)	0.96
	Coarse fraction of sand (%)	0.0
	Medium fraction of sand (%)	90.4
	Fine fraction of sand (%)	9.0
	Maximum dry unit weight ($\gamma_{d,max}$) (kN/m^3)	16.95
	Minimum dry unit weight ($\gamma_{d,min}$) (kN/m^3)	14.52
	Frictional angle (φ^o) at D_r = 35%	38.8^0
	Frictional angle (φ^o) at D_r = 70%	40.5^0
	Frictional angle (φ^o) at D_r = 90%	41.5^0

The sand is classified as poorly graded sand (SP) as per the Unified Soil Classification System (USCS). The shear strength parameters of sand at different relative densities (Dr = 35, 70 & 90%) were determined by the direct shear method [54]. A direct shear box of dimension 60 mm × 60 mm × 30.2 mm (length × breadth × height) was used to find out the shear strength parameters of the sand. The stress-strain responses obtained from the direct shear tests on the dry samples at relative densities of 35, 70, and 90% are shown in Fig. 3.3, Fig. 3.4, and Fig. 3.5, respectively. The peak friction angle (φ) of the sand, at these relative densities, are obtained as 38.80, 40.50, and 41.50, respectively. The plot of normal stress versus peak shear stress is presented in Fig. 3.6.

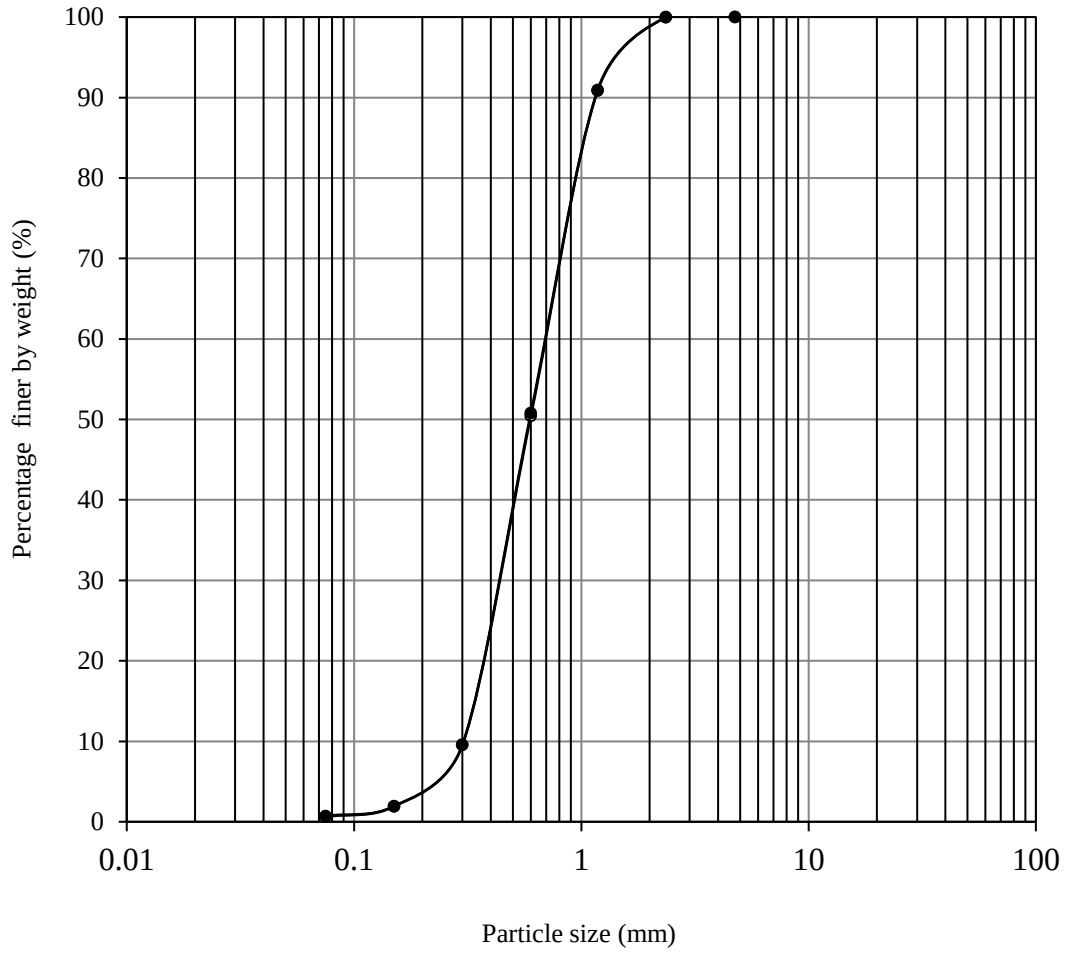

Fig. 3.2 Particle size distribution of the Brahmaputra river sand used.

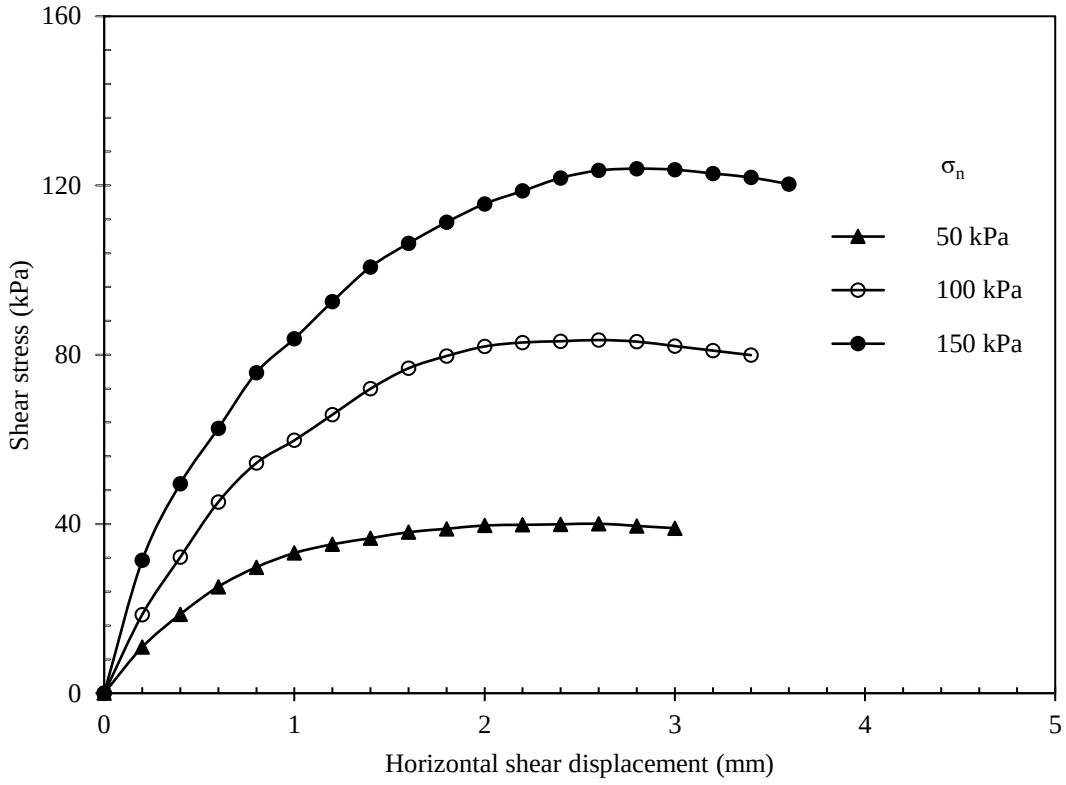

Fig. 3.3 Shear stress-horizontal shear displacement response of sand (D_r = 35%) in direct shear test

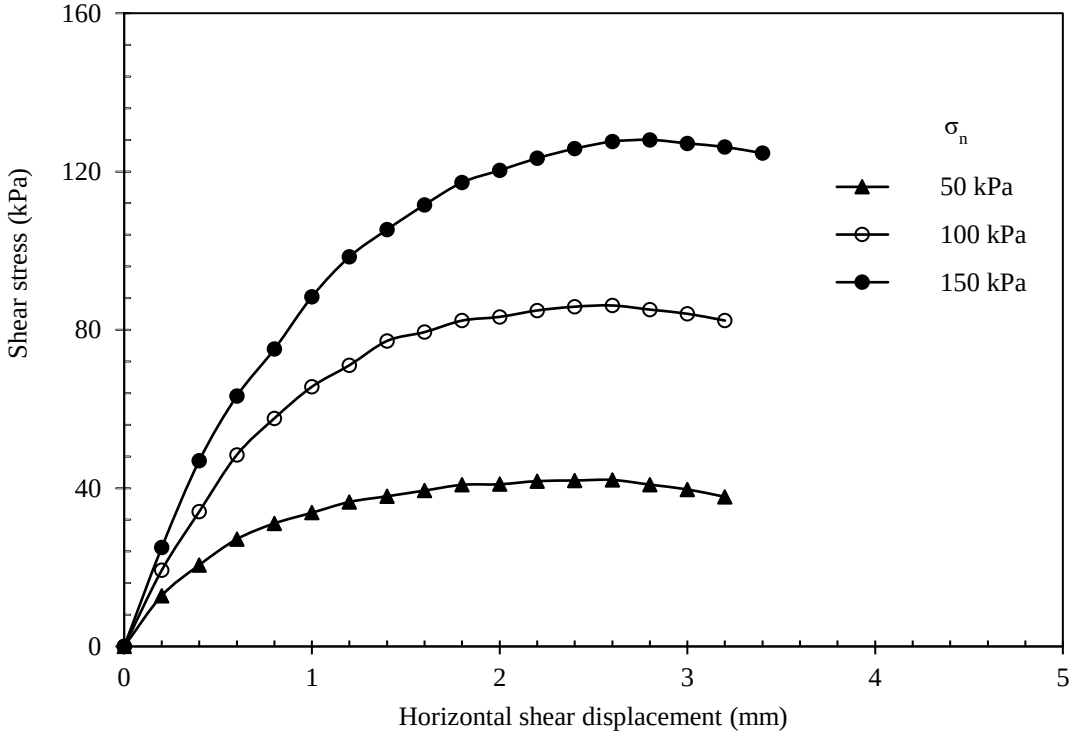

Fig. 3.4 Shear stress-horizontal shear displacement response of sand (D_r = 70%) in direct shear test

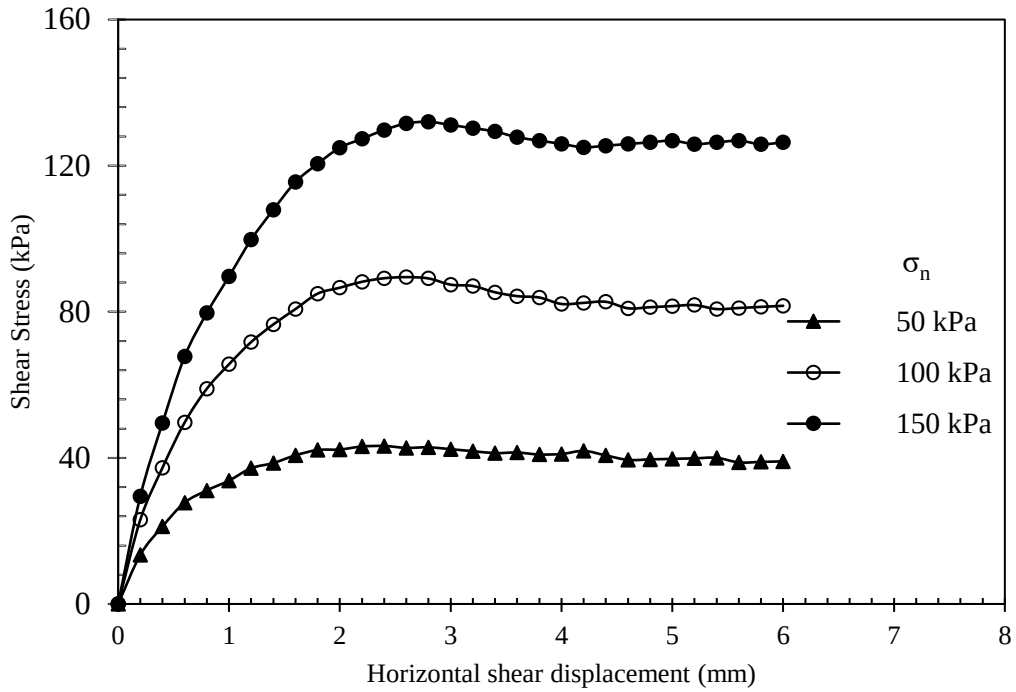

Fig. 3.5**:** Shear stress-horizontal shear displacement response of sand (D_r = 90%) in direct shear test

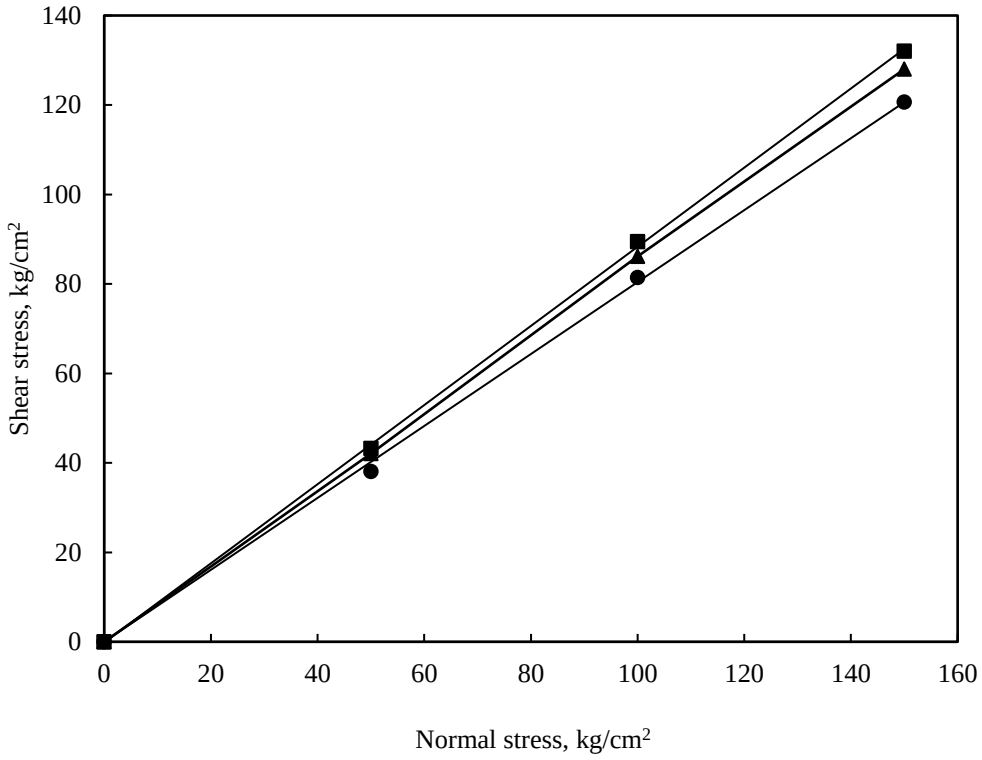

Fig. 3.6 Normal stress-peak shear stress response of sand in direct shear for different relative densities

3.2.2 Geocell reinforcement

The geocell was prepared in the laboratory by stitching polyester woven geotextile. This material is abundantly available in the form of common office curtain blinds. To fabricate the geocell of the desired dimension, paper templates were first made. The geotextile was then cut and stitched with nylon thread as per the template. The tensile stress-strain behavior of the geotextile used for the geocell is shown in Fig. 3.7 [3]. The material properties of the geotextile used were tested in the laboratory and the results are shown in Table 3.2. The prepared geocell seam was also tested and was found to be as strong as the parent material. A photographic view of the geotextile, the stitching process to form the geocell, one dimension of the geocell pocket, and the complete form of the geocell reinforcement are shown in Fig. 3.8(a-d).

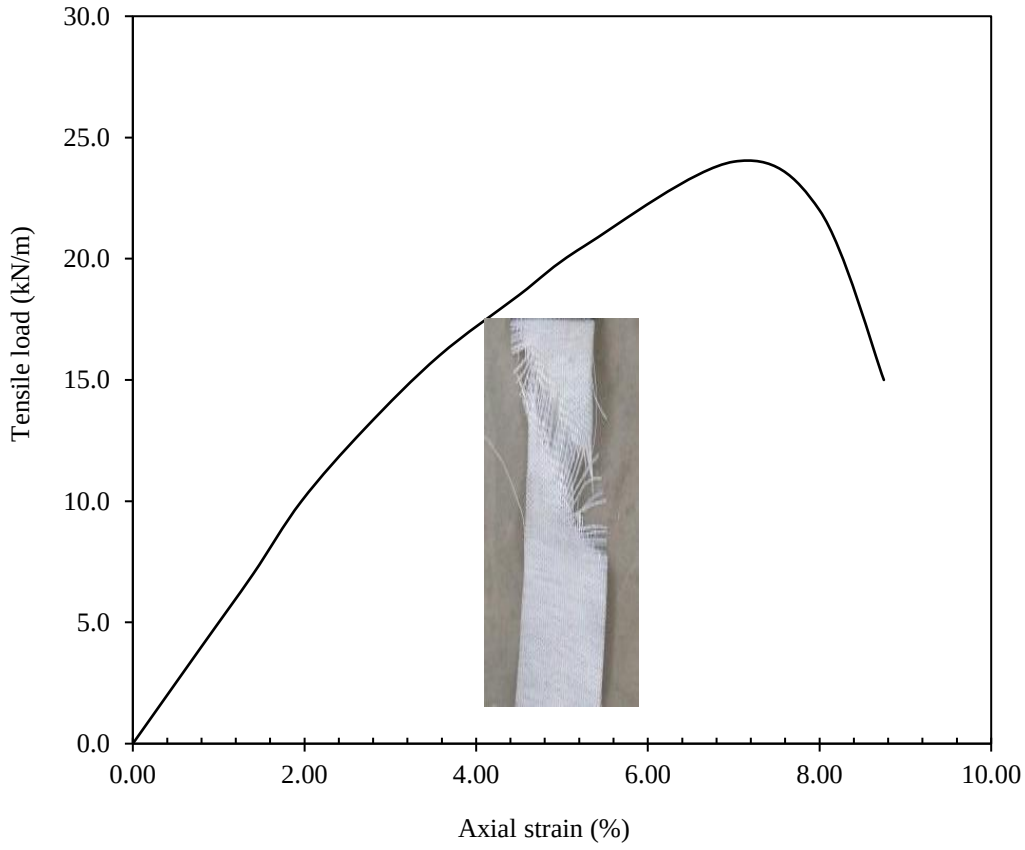

Fig. 3.7 Tensile stress vs strain response of the curtain blind used for geocell

Table 3.2 Properties of the curtain blind used to make the geocell

Parameter	**Description**
Geocell material type	Woven geotextile
Polymer	Polyester
Thickness, t (mm)	0.8
Ultimate tensile strength, T_u (kN/m)	24
Strain at failure, ε_u (%)	7.0
Secant modulus at 2% strain, $J_{s=2\%}$ (kN/m)	500
Secant modulus at 5% strain, $J_{s=5\%}$ (kN/m)	400
Secant modulus at failure, $J_{s=7\%}$ (kN/m)	343
Cell seam strength (kN)	2.2

Note: The ultimate tensile strength of PP Geogrids is 20 kN/m as per IS 17371: 2020 [51] and this is comparable to the tensile strength of curtain blind used in this study.

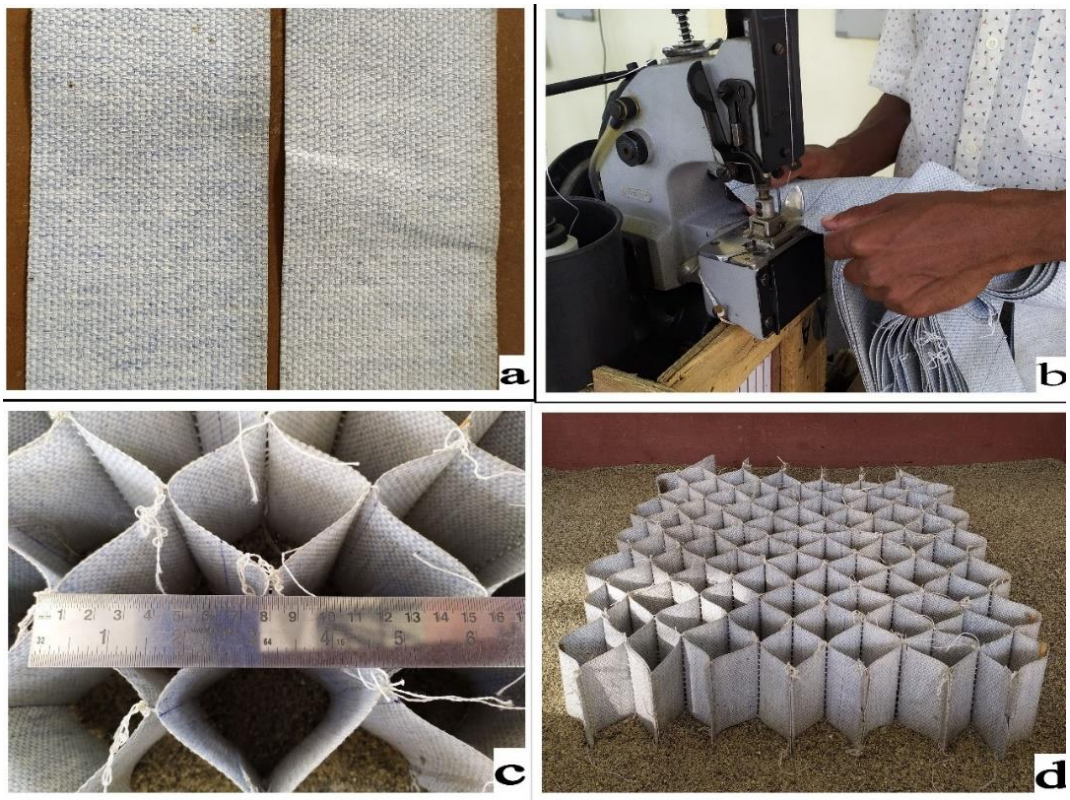

Fig. 3.8 Photographic view of (a) curtain blind; (b) stitching of curtain blind; (c) one dimension of geocell pocket; (d) curtain blind geocell after complete stitching

The interfacial frictional property of the geotextile was also determined through a direct shear test as per IS: 2720 (Part 13) 1986 [54], for different relative densities of sand (i.e., 35%, 70%, and 90%). However, a comparative study was carried out by conducting direct shear test as per IS 17483 Part 1 2020 [52] and non-clamping geocell, IS: 2720 (Part 13) 1986 [54]. It was observed that by conducting direct shear test without clamping give slightly higher interfacial friction angle (< 4%) as compared to standard procedure [52]. Since in actual condition the frictional resistance was experienced by both surfaces of the cells (inner and outer surface), and hence the direct shear test was conducted without clamping [54]. The geotextile layer was placed in the shear plane (soil-geotextile-soil) of the direct shear box (Fig. 3.9). The stress-strain responses obtained from the direct shear tests on dry sand-geotextile for the cases of D_r = 35%, 70% and 90% are shown in Fig. 3.10, 3.11 and 3.12 respectively. The interfacial friction angle (δ_s) of the sand – geotextile, at these relative densities are found to be 38^0, 39.8^0, and 41.4^0 respectively. Summaries of the results of sand-geotextile interface tests are presented in Table 3.3

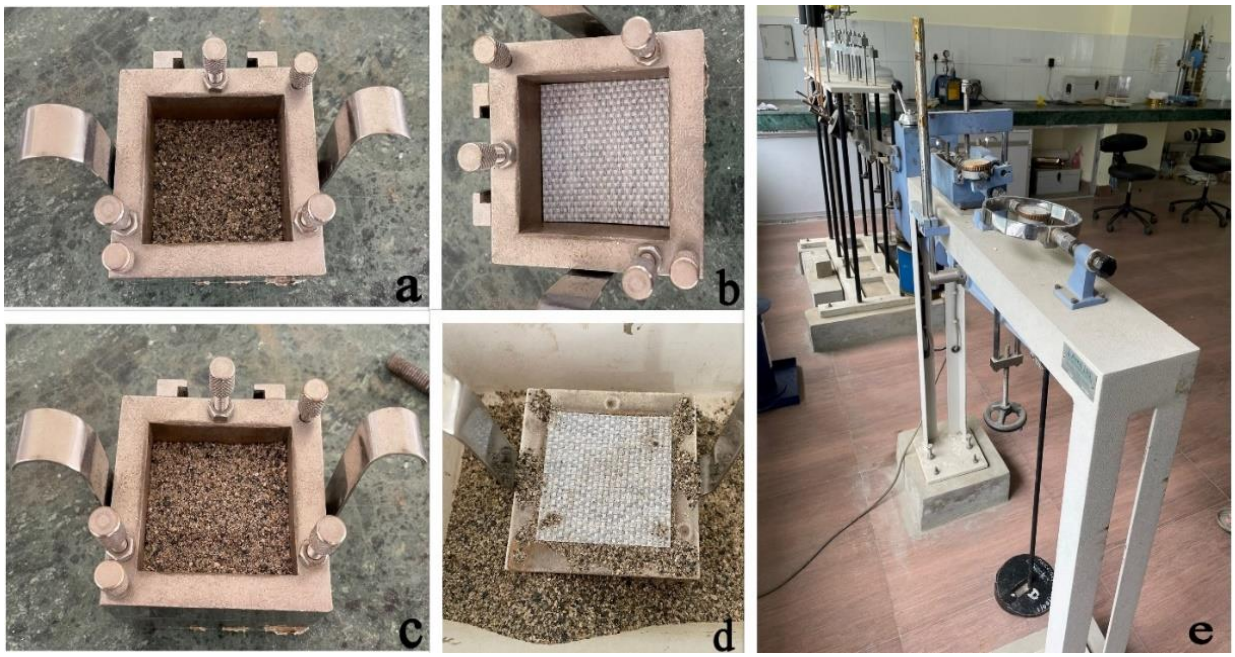

Fig. 3.9 Photographic view of (a-b-c) soil-geotextile-soil layer in the direct shear box; (d) bottom layer of soil with geotextile in the direct shear box after the test; (e) direct shear apparatus with the prepared sample.

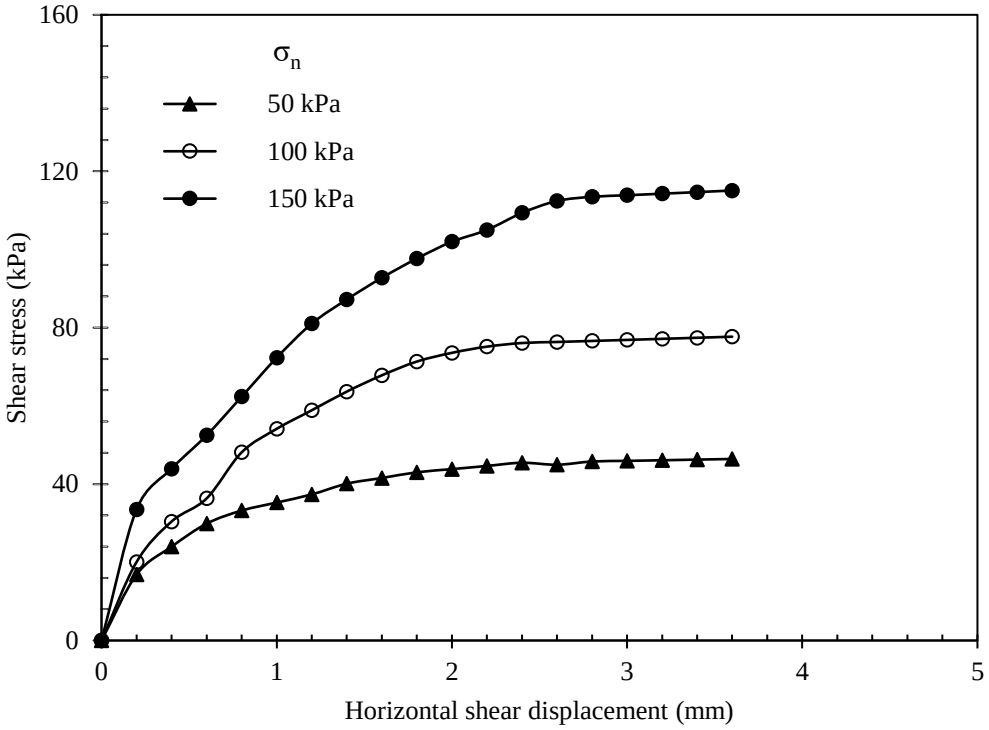

Fig. 3.10 Shear stress-horizontal shear displacement response of sand (D_r = 35%) in direct shear test

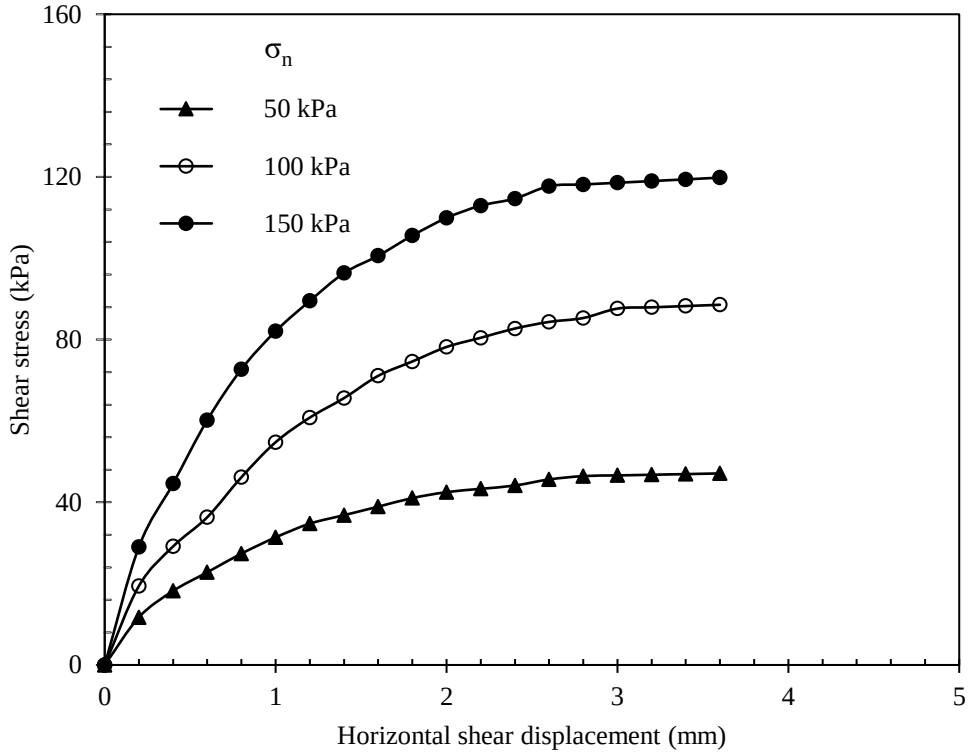

Fig. 3.11 Shear stress-horizontal shear displacement response of sand (D_r = 70%) in direct shear test

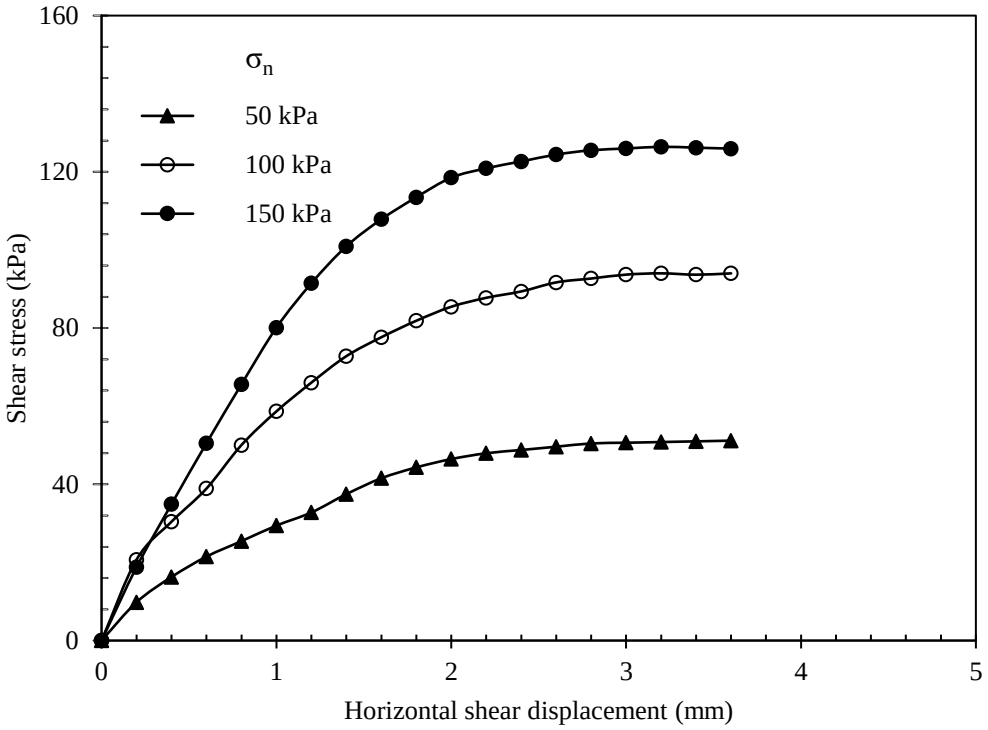

Fig. 3.12 Shear stress-horizontal shear displacement response of sand (D_r = 90%) in direct shear test

Table 3.3 Summary of test results for different relative densities of sand–geotextile interfaces by direct shear test.

Type of interface	Normal stress, σ_n (kPa)	Shear stress τ (kPa)			Interfacial friction angle δ_s (^{0})		
		D_r 35%	D_r 70%	D_r 90%	D_r = 35%	D_r = 70%	D_r = 90%
Soil-soil	50	38.1	42.1	43.3	38.8	40.5	41.5
	100	81.5	86.1	89.5			
	150	120.6	128.0	132.0			
Sand-geotextile	50	46.4	46.6	51.2	38.0	39.8	41.4
	100	77.7	88.3	94.0			
	150	115.1	119.8	126.4			

3.3 Experimental programme

In the experimental study, tests were carried out systematically under various series to examine the influence of different geocell-geometric parameters on the performance of geocell-reinforced sand under square footing upon application of static and repeated loading. The effect of the shape of footing (square, strip, rectangular) on the performance of unreinforced and geocell-reinforced sand under static loading was also investigated. The homogeneous foundation beds of the small-scale model tests were prepared in a rectangular mild steel tank. In each series of the study, only one parameter was varied keeping the others constant, to investigate the effect of that particular parameter on the overall behaviour of the foundation. The complete description of the test series is summarized in Table 3.4. All the parameters are expressed in a non-dimensional form concerning the footing width (B). The optimum value obtained from a given series of tests was adopted in the next series of tests.

The test series A was conducted on an unreinforced sand bed of D_r = 70% for different shapes of footing under static loading. In series B1 and B2, tests were carried out on an unreinforced sand bed of different relative densities (D_r = 35, 70, and 90%). In these tests, the square footing was used under static and repeated loading.

Test series C1, C2, D1, D2, E1, E2, F1, and F2 were carried out on the geocell-reinforced sand bed at medium dense state (D_r = 70%) under both static and repeated loading. The square footing was used to investigate the performance improvement of the geocell-reinforced sand bed. The parameters studied in these tests include geocell-pocket size, geocell height, the width of geocell reinforcement, and placement depth of the geocell layer. Based on the results from these tests, optimum geocell-geometric parameters giving the maximum performance improvement were determined.

Test series G1 and G2 were conducted to evaluate the influence of the relative density of subgrade sand on the performance of geocell-reinforced sand beds under static and repeated loading. Test series H was carried out to investigate the influence of infill soil density on the performance of geocell reinforced sand bed under static loading. The test series under I was performed on geocell-reinforced sand beds of three different shapes of footing (square, strip, rectangular) under static loading.

Table 3.4 Schedule of model scale tests

Test Series	Reinforcement	Test parameters		No of tests
		Variable	**Constant**	
A	Unreinforced	Square Strip Rectangular	D_r = 70%, Monotonic loading	3+3*
B1	Unreinforced	Relative Density of subgrade sand (D_r) 35%, 70% and 90%	Square footing, Monotonic loading	2+2*
B2			Square footing, [1]Repeated loading	3+3*
C1	Geocell	u/B = 0, 0.1, 0.25, 0.5 and 1	d/B = 0.5, h/B = 0.66, b/B = 3, D_r = 70% & $D_{r,\ infill}$ = 70%, Square footing, Monotonic loading.	5+2*
C2			d/B = 0.5, h/B = 0.66, b/B = 3, D_r = 70% & $D_{r,\ infill}$ = 70%, Square footing, q_d = 91 kPa & 150 kPa, Repeated loading	10+2*
D1	Geocell	d/B = 0.33, 0.50, 0.75, 1 and 1.5	h/B = 0.66, b/B = 3, u/B = 0.10, D_r = 70% & $D_{r,\ infill}$ = 70%, Square footing, Monotonic loading.	4+2*
D2			h/B = 0.66, b/B = 3, u/B = 0.10, D_r = 70% & $D_{r,\ infill}$ = 70%, Square footing, q_d = 91 kPa & 150 kPa, Repeated loading	8+2*
E1	Geocell	h/B = 0.33, 0.50, 0.66, 1 and 1.25	d/B = 0.5, b/B = 3, u/B = 0.10, D_r = 70% & $D_{r,\ infill}$ = 70%, Square footing, Monotonic loading.	4+2*
E2			d/B = 0.5, b/B = 3, u/B = 0.10, D_r = 70% & $D_{r,\ infill}$ = 70%, Square footing, q_d = 91 kPa & 150 kPa, Repeated loading	8+2*
F1	Geocell	b/B = 1, 2, 3, 4, 5 and 6	d/B = 0.5, h/B = 0.66, u/B = 0.10, D_r = 70% & $D_{r,\ infill}$ = 70%, Square footing, Monotonic loading.	5+2*
F2			d/B = 0.5, h/B = 0.66, u/B = 0.10, D_r = 70% & $D_{r,\ infill}$ = 70%, Square footing, q_d = 91 kPa & 150 kPa, Repeated loading	10+2*
G1	Geocell	Relative Density of subgrade sand (D_r) 35% & 90%	d/B = 0.5, h/B = 0.66, u/B = 0.10, b/B = 1, 2, 3, 4, 5 and 6 & $D_{r,\ infill}$ = 70%, Square footing, Monotonic loading.	12+4*
G2			d/B = 0.5, h/B = 0.66, u/B = 0.10, b/B = 3 & $D_{r,\ infill}$ = 70%, Square footing, q_d = 91 kPa & 150 kPa, Repeated loading	4+2*
H	Geocell	Relative Density of infill sand ($D_{r,\ infill}$) 35%, 70% & 90%	d/B = 0.5, h/B = 0.66, u/B = 0.10, b/B = 3, D_r = 70%, Square footing, Monotonic loading.	2+2*
I	Geocell	Square Strip Rectangular	d/B = 0.5, h/B = 0.66, u/B = 0.10, b/B = 3, D_r = 70% & $D_{r,\ infill}$ = 70%, Monotonic loading	2+2*
J1	Unreinforced	q_d/q_{ult} = 20%, 40%, 70% and 85%	D_r = 70%, Square footing, Repeated loading.	4+2*
J2	Geocell	q_d/q_{ult} = 20%, 40%, 70% and 85%, and q_d = 64 kPa	d/B = 0.5, h/B = 0.66, u/B = 0.1, b/B = 3, D_r = 70% & $D_{r,\ infill}$ = 70%, Square footing, Repeated loading.	4+2*

[1]Repeated loading: Ultimate bearing capacities of unreinforced sand with relative densities 35%, 70% and 90 % are considered as the maximum magnitude of repeated loads (i.e. 58 kPa, 91 kPa & 128 kPa) for unreinforced soil.

*The tests which were performed two or three times to verify the repeatability of the test data.

Test series J1 and J2 were conducted on unreinforced and geocell-reinforced sand beds for the different magnitudes of repeated loading.

3.4 Test description

3.4.1 Test set-up

The internal dimensions of the steel tank that was fabricated for the experimental study were 1200 mm × 980 mm × 1010 mm (length × breadth × height). Structural steel angle sections were welded to connect the test tank side plates to achieve negligible lateral deformation. A reaction steel frame, designed to support a 100-kN hydraulic jack, was attached to the steel tank (Fig. 3.13).

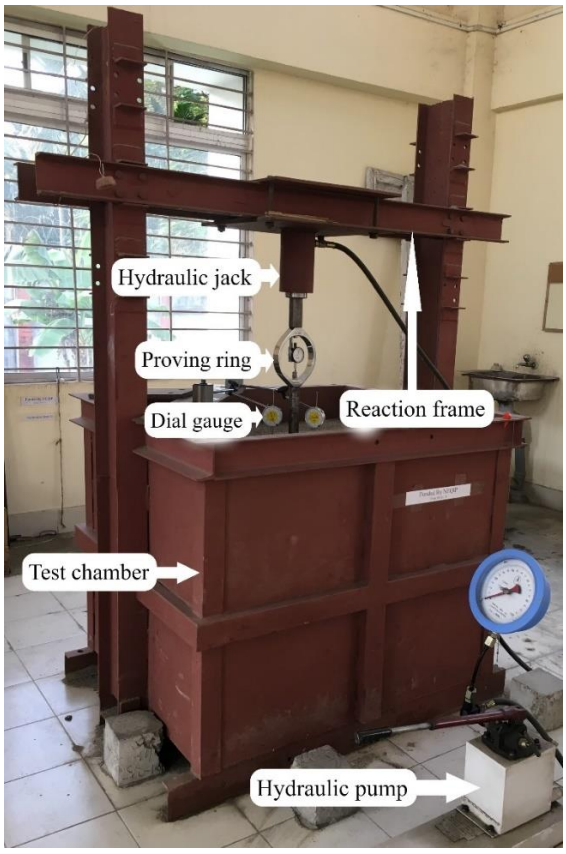

Fig. 3.13 Photograph of laboratory model test setup

Three types of model footing were used in the study as described below-

(a) Square model footing- 150 mm ×150 mm × 20 mm (L ×B × t)

(b) Strip model footing- 975 mm ×150 mm × 20 mm (L ×B × t) with crane rail CR50 rail to avoid buckling of model footing (Fig. 3.11).

(c) Rectangular model footing- 200 mm ×150 mm × 20 mm (L ×B × t)

A thin layer of sand was pasted to the bottom face of the steel plates to make them rough. The dimension of the test tank and the size of the loading plate were determined based on the literature. Chummar [19] suggested that in the case of cohesionless soil, the failure wedge was likely to be extended to a maximum of about 3*B* (*B* is the width of footing) distance on either side of the footing centre line and a depth of about 1.1*B* from the footing bottom. Therefore, in the present study, the foundation bed width/length (980 mm/1200 mm) of 6.533*B*/8.0*B* and depth (880 mm) of 5.867*B* was considered large enough to avoid the boundary effects, and hence the experimental results. The model tests were performed by manually operated hydraulic loading. The model footings were subjected to a reaction load applied vertically through a steel ball. The reaction load applied through the hydraulic jack to the footings was controlled manually and was measured with a pre-calibrated proving ring. The loading arrangement is illustrated in Fig. 3.14. The settlements of the footing were measured with two dial gauges placed on the model footing diagonally opposite to each other. The surface deformations (heave) were measured by using four dial gauges placed on the foundation soil at distances 1.5*B* and 3*B* from the centre on either side of the footing (Fig. 3.15).

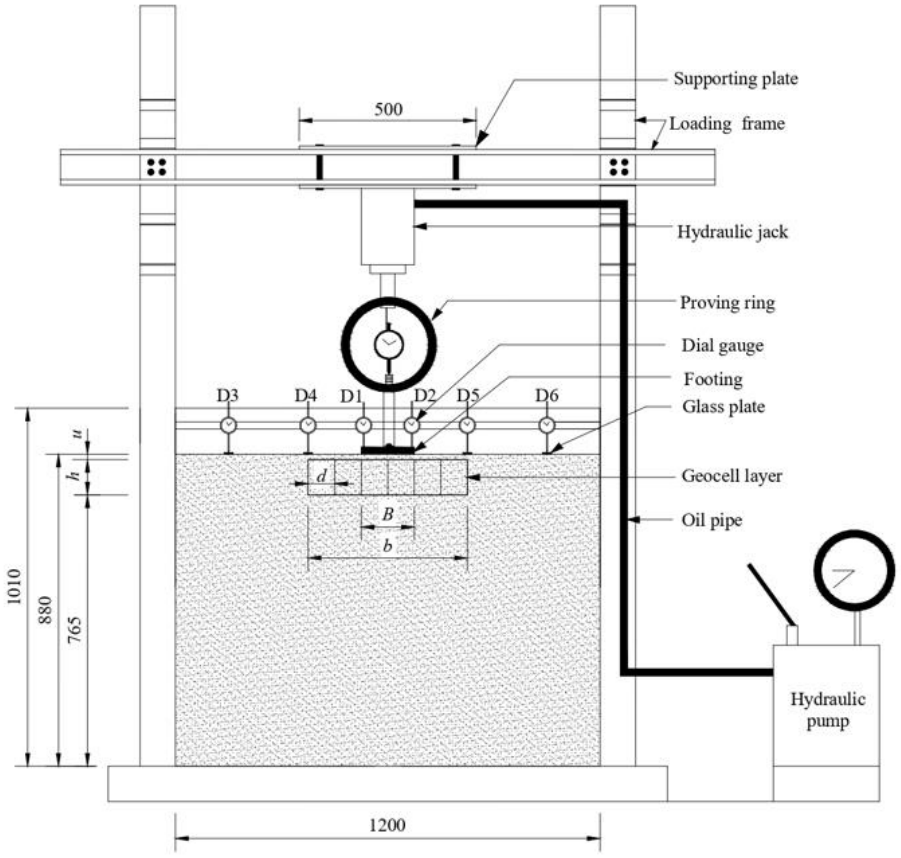

Fig. 3.14 Test setup scheme (Note: All dimensions are in mm)

Fig. 3.15 Photograph of dial gauge arrangements for deformation measurement of the sand bed

3.4.1.1 Monotonic load/Static load tests

Static load tests were carried out as per IS 1888- 1982 [57]. After the experimental set-up was ready, the load was applied in cumulative increments up to one-fifth of the estimated ultimate bearing capacity. The loads were applied without impact, fluctuation, or eccentricity and the loads were measured with a pre-calibrated proving ring. The settlements of the footing were observed for each increment of the load till the rate of settlement became negligible. The next increment of the load was then applied and observations were repeated. The test was continued till a settlement of 22% of the footing size was achieved or the soil bed failed under shear.

For all the static tests, settlement versus load curves was plotted. The ultimate bearing pressure (q_U) for the unreinforced sand was compared with the ultimate bearing pressure of reinforced sand (q_R), and the improvement factor, IF $= \frac{q_R}{q_U}$ was calculated for all the tests. Another parameter, known as the percentage reduction of settlement (*PRS*), was used to express the decrease in settlement under reinforced conditions. $PRS = (1 - \frac{s_R}{s_U})$, where s_R indicates the settlement in a reinforced condition at a bearing pressure

corresponding to the ultimate bearing pressure of the unreinforced sand and s_U represents the settlement corresponding to the ultimate bearing capacity of unreinforced condition. The relationship between pressure and settlement obtained from the tests was studied by plotting curves for all the tests of the series conducted. Further, pressure vs surface deformation for all the tests was studied at different settlement levels for all the tests of the series performed.

3.4.1.2 Repeated load tests

After the set-up has been arranged, the initial readings of the dial gauges were noted and the first increment of the static load was applied to the footing. In the case of 1st cycle of loading, the load was increased from zero to pre-determined values of 20%, 40%, 70% & 85% of ultimate bearing capacities for unreinforced/reinforced sand in nearly five small increments. Each load increment was maintained until the rate of settlement of the footing was reduced to 0.02 mm/min. In the unloading process, the load was reduced from the maximum applied value to zero in 15 minutes and the settlement was recorded when the rate of settlement of the footing was reduced to 0.02 mm/min. This process of 1st cycle of loading-unloading took about 300 minutes. Thereafter, subsequent cycles of reloading and unloading were applied on the footing which was termed repeated loading.

The repeated load tests were conducted on unreinforced and geocell-reinforced sand beds to study the influence of different geocell geometric parameters, the relative density of subgrade sand, and different magnitudes of repeated loading on its performance. A typical load settlement curve is shown in Fig. 3.16.

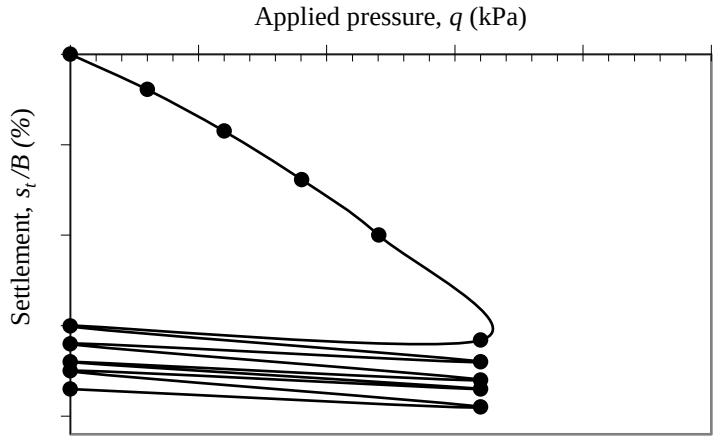

Fig. 3.16 Typical load-settlement curve for cyclic plate load test

3.5 Preparations of test specimens and procedure

3.5.1 Preparation of sand bed

Sand beds were prepared using the pluviation technique (raining sand through the air). The Schematic diagram and photograph of the sand raining device are shown in Fig. 3.17. It is an assembly of a large hopper (sand container) and a 700 mm long hollow pipe having a 60° inverted cone connected at the bottom. The density obtained through the rainfall technique depends on the height through which the sand is allowed to fall. The system was calibrated by measuring the respective density achieved for different preset heights of fall during a pluviation test series. The calibration curve showing the relationship between the height of the fall and the corresponding relative density is shown in Fig. 3.18. Based on this calibration curve, the height of fall corresponding to the required relative density was adopted to form the test beds. To verify the accuracy and consistency of the density of sand, small containers of known volumes were placed at different locations in the test tank. By this technique, less than $\pm 5\%$ variation was observed in the measured densities at different locations of the sand bed.

The geocell reinforcement fabricated as explained in section 3.2.2, was placed on the desired level of the sand bed and their pockets were filled with the sand pluviation technique. The sand was rained from a pre-determined height to obtain the desired relative density (Fig. 3.17).

3.5.2 Test procedure

The tests were carried out by using model footings placed at the centre of the tank. In model footings, a thin layer of sand was pasted to the bottom face of the steel plates to make it rough. Before placing the steel plate footing, the final sand surface over the geocell was leveled, taking care to avoid a change in density. The footing and the ram of the hydraulic jack were aligned with the centre of the tank to apply static or repeated loading. The dial gauges were placed at suitable locations; at distances *B,* 2*B,* and 3*B* from the centre and on either side of the footing (Fig. 3.14). The footing was loaded with a hydraulic jack as described in section (s) 3.4.1.1 and 3.4.1.2. During loading, deformations from the dial gauges and load in the proving ring were recorded at different intervals of footing settlements. The loading was continued till a settlement of about 22%

of the footing width was reached in static load tests. The repeated load tests were carried out for 20 cycles of repeated loads except for a few cases where 35 cycles were applied.

The test bed for each test was prepared afresh with new reinforcement. The results obtained are presented and discussed in the following chapters.

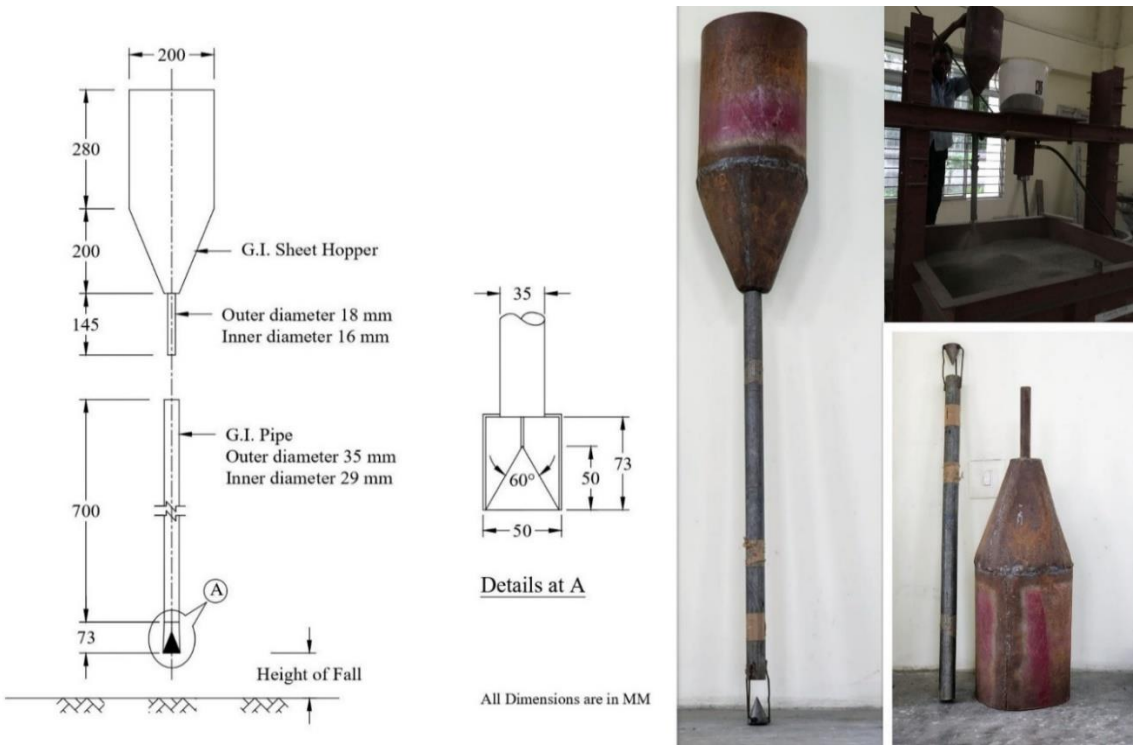

Fig. 3.17 Schematic diagram and photograph of the sand raining device

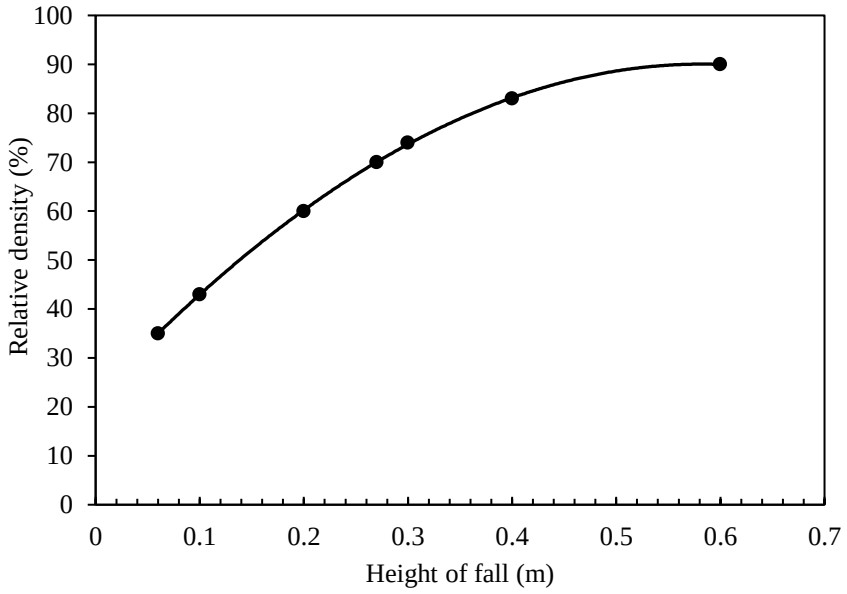

Fig. 3.18 Calibration curve for a height of fall versus relative density